Peculiarities of superconductivity in the single-layer FeSe/SrTiO_{3} interface

Lev P. Gor'kov

Phys. Rev. B **93**, 060507 — Published 12 February 2016

DOI: 10.1103/PhysRevB.93.060507

On peculiarities of superconductivity in the single-layer $FeSe/SrTiO_3$ interface

Lev P. Gor'kov[1,2]

[1]*NHMFL, Florida State University, 1800 E. Paul Dirac Drive, Tallahassee, Florida, 32310, USA*
[2]*L.D. Landau Institute for Theoretical Physics of the RAS, Chernogolovka, 142432, Russia*

(Dated) PACS number(s): 74.78.−w, 74.25.F−, 74.62.-c, 71.38.-k

Observation of replica bands in the ARPES spectra of single-layer FeSe on strontium titanate substrate revealed a phonon component contribution to mechanisms behind its high T_C superconductivity. We study the interaction of the in-layer FeSe electrons with the electric potential of the longitudinal (LO) modes at the surface of bulk $SrTiO_3$. A two-dimensional system of charges at the $FeSe/SrTiO_3$ interface includes both the itinerant and immobile electrons. The latter change significantly the interface characteristics, increasing screening at the substrate surface and thereby reducing the strength of the electron-LO phonon interaction. In what follows, the dielectric constant serves as a free parameter and is determined using the ARPES measurements of the replicas. Two-dimensional Coulomb screening is accounted for in the random phase approximation. It is shown that the model is applicable overthe entire range of the parameters typical for current experiments. The estimates from this model make possible the conclusion that the LO-phonon mediated pairing alone cannot account for the temperatures of the superconducting transitions T_C in the single-layer $FeSe/SrTiO_3$ reported in these experiments. This does not exclude that the LO-phonons mechanism can become more significant in differently and better prepared single layer FeSe films. Available experiments are briefly discussed. Thus far no measurements exist on the dependence of T_C on the concentration of electrons doped into the in-layer FeSe band.

Introduction. The recent discovery of superconductivity in a single layer of FeSe deposited on a strontium titanate substrate (STO) [1] with superconducting transition temperatures up to 110K [2] is of great interest both on practical and on theoretical grounds. On the practical side, it opens new prospects in applications, including, in particular, the engineering of interfaces and films exhibiting superconductivity. On the theorical side, the whole manifold of experimental data reveals evidence that a phonon mechanism is undoubtedly at work, thereby challenging the forty-years-old consensus in the literature regarding stringent limitations on superconducting transition temperatures of the achievable with phonons [3].

In what follows, we undertake attempts to reveal the basic factors that control both the normal and superconducting properties of single-layer FeSe/STO. Observation of replica bands in angle-resolved photoemission spectroscopy (ARPES) data [4, 5] made self-evident the coupling between electrons and a high frequency surface phonon mode. In general terms, the idea that surface modes may be responsible for pairing between the in-layer FeSe electrons was of course put forward in the literature. To be specific, we focus on the interaction of electrons with the longitudinal (LO) surface polar modes on the charged STO substrate.

This problem cannot be addressed without making some suppositions regarding the structure of the interface and the mechanisms responsible for the electronic doping of the FeSe-layer. In current experimental literature [1, 2, 4-9] the procedures for sample preparation begin with annealing the substrate in a vacuum in order to produce oxygen vacancies and to form, thereby, a charged two-

dimensional layer at the $SrTiO_3$ surface. The unit-cell-thick FeSe layer is then deposited by molecular beam epitaxy (MBE). It seems that only a fraction of the charges are transferred into the conduction band of the single FeSe layer after the deposition. The rest stay on the surface of $SrTiO_3$ [5-7, 9 and 10]. While solution of the problem of electrons interacting with the electric fields inherent in LO polar modes on the surface of a *dielectric* is well known [11], in the present case it becomes complicated by changes in the dielectric properties of the surface caused by the immobile charge remaining on the substrate. The presentation below is an attempt to account for these peculiarities in the phenomenological model by generalizing the standard approach [11].

Although from observation of the replica bands [4] one can infer that the interaction between electrons and the surface optical phonons is among the key features in the system, there remains the question whether the mechanism of the LO phonon-mediated pairing alone can lead to so high a T_c as observed in single-layer FeSe/STO (1UCFeSe/STO) [2]. In the framework of our suggested approach we derive the expression for the intensity of the replica bands that makes it possible to analyze measurements [4] quantitatively. Within the range of parameters revealed by this analysis the answer is negative. This conclusion agrees with the one in [4]. Nevertheless, when acting in concert with other mechanisms, the contribution from the LO surface phonons is found capable of significantly enhancing T_c compared to its value in bulk FeSe. Note in passing that the particular mechanism of superconductivity in the latter is currently under debate (see, e.g. [12, 13]).

*The model.*Assume for the start that the interaction of electrons with a high frequency optical surface mode is the sole mechanism of superconductivity in this system. With that assumption, the main unconventional theoretical feature is the inverted ratio between the Fermi energy E_F and the characteristic LO phonon frequency. In traditional metals the typical frequency ω_0 of the phonons contributing to pairing has the same order of magnitude as the Debye temperature. The latter usually equals a few hundred Kelvin and is some two orders of magnitude smaller than E_F which is of order of $1eV$. This results in a transition temperature that is also rather small, of order one tenth θ_D, (a few Kelvin). In lead (Pb) $T_C \approx 7.2K$. $T_C \sim 10^{-2}\theta_D$ typical for most metals of the main groups. For the material of interest here, single layer FeSe/STO, $E_F \approx 60meV$, $\omega_0 \approx 80meV$ and T_C is between $50K$ and $100K$ [2, 4 and 9]. from in Lead (Pb) that is

The ratio $T_C / \omega_0 \approx 1/8$ (with $T_C \approx 110K$ [2]) suggests that interactions in the system responsible for pairing are not weak. In metals the extension of the BCS weak coupling model to the case of arbitrarily strong interactions is realized by the set of the well- known Eliashberg equations [14]. However, these equations are applicable only in the so called adiabatic limit, that is, at the condition that the Migdal parameter $r = \omega_0 / E_F$ is small $\omega_0 << E_F$ [15].

With the Migdal adiabatic provision severely violated in the new system, the discussions below must inevitably acquire a qualitative character. In a crude approximation, however, one might formally consider that the one eighth ratio of $T_C / \omega_0 \approx 1/8$ is caused by a suffuciently small coupling parameter λ in the BCS-like expression for the temperature of the superconducting transition:

$$T_c = const \times W(2\gamma/\pi)\exp(-1/\lambda) . \quad (1)$$

We show below that the electron-optical phonon interactions mechanisms cannot explain $T_C \approx 100K$, so indeed the corresponding coupling parameter λ must be small. Accordingly, for single-layer

FeSe/STO we adopt an idealized weak coupling model for the two-dimensional parabolic band of electrons at the M-point of the Brillouin zone (BZ) [4,5 and 9]. For simplicity's sake, we begin by assuming the *extreme* "anti-adiabatic" case $\omega_0 >> E_F$.

Interaction of two-dimensional electrons with longitudinal surface optical phonons. Interaction between electrons and the electric potential generated by LO phonons in polar crystals is described by the Fröhlich Hamiltonian:

$$\vec{P} = F_C \vec{u} \quad (2)$$

where $\vec{P}$ and $\vec{u}$ are the polarization and the lattice displacement, respectively. In particular, the well-known case is the interaction between the surface optical phonons and electrons on the surface of a *clean* dielectric [11]. The coefficient F_C equals:

$$\overline{F}_{C,i} = \left[4\pi e^2 \frac{\hbar \omega_{SLO}^j}{2} \left(\frac{1}{\kappa_\infty + 1} - \frac{1}{\kappa_0 + 1} \right) \right]^{1/2} . \quad (3)$$

κ_0 and κ_∞ are the static and the optical dielectric constants of the bulk. In (3) ω_{SLO}^j is the frequency of one of the SLO phonon modes. The matrix element for the scattering of two electrons via virtual exchange of a surface phonon is:

$$M_i(q) = -\frac{4\pi e^2}{q} \left(\frac{1}{\kappa_\infty + 1} - \frac{1}{\kappa_0 + 1} \right) \times D_{SOP}^i(q) \quad . (4)$$

In Eq. (4) $D_{SOP}^i(q)$ is the phonons Green function in the thermodynamic technique [16]:

$$D_{SOP}^i(q)(\varepsilon_n - \varepsilon_m) = \frac{(\omega_{SLO}^j)^2}{(\omega_{SLO}^j)^2 + (\varepsilon_n - \varepsilon_m)^2} . \quad (5)$$

In (4,5) $\vec{q} = \vec{p} - \vec{k}$ and $\varepsilon_n - \varepsilon_m$ are the momentum and the frequency that two electrons exchange upon scattering. In bulk, the well-known relation between ω_{LO} the frequency of the LO and the frequency ω_{TO} of the soft transverse optical phonons is $\omega_{LO} / \omega_{TO} = \sqrt{\kappa_0 / \kappa_\infty}$; according to [11], and from here the frequency ω_{SLO} of the surface phonon $\omega_{SLO} / \omega_{TO} = \sqrt{\kappa_0 + 1 / \kappa_\infty + 1}$.

As mentioned in introduction, for the problem in hand inconsistencies between experimental results and their interpretation seem to come about from incomplete understanding of the doping mechanisms. Without entering into excessive details of awhat is the customary doping protocol, it is worthwhile to enumerate the main steps. A carefully prepared TiO_2-terminated $SrTiO_3$ substrate is annealed in vacuum at high temperature, thereby creating oxygen vacancies at its surface and forming a charged surface layer hosting a two-dimensional electron system on the titanium *3d* t_{2g}–levels [1, 2, 4-9]. It is worthwhile to note that the layer of FeSe is deposited by molecular beam epitaxy (MBE) *after*, i.e., on top of an *annealed surface*. A fraction of the electrons from the charged $SrTiO_3$ surface go over into the single-layer FeSe conduction band; however, some undoubtedly remain embedded in a thin surface layer on the substrate. Experimentally, it is firmly established that the results do not

depend on whether $SrTiO_3$ is insulating in bulk or Nb-doped. From this also follows the corollary that the conducting FeSe layer and the interfaces make a whole (see e. g. [5-7]).

The experimental discovery , consistent with the above considerations, that finalizes the model is the disclosure of a threshold in concentration for the doped carriers to appear at the chemical potential [6-8]. Such a threshold signifies the existence of the mobility edge; only at concentrations above the threshold can the carriers start manifesting themselves in itinerant conductivity and superconductivity. Whether the concentration for the onset of the threshold can be controlled by a specific annealing protocol remains unclear from [8], but the very fact that such a threshold exists is critically important. At concentrations exceeding the threshold the itinerant and immobile carriers coexist and it becomes necessary to keep in mind that all phenomena in the conducting 1UCFeSe/STO-interface take place on a reconstructed dielectric background. Because the dielectric constant κ_0 of $SrTiO_3$is very large ($\kappa_0 = 1000$ at $T = 100K$ [17]), the local states below the mobility edge possess large dipole moments that contribute significantly into the polarization.

Below we *hypothesize* that the interactions between two-dimensional electrons and the optical phonons in 1UCFeSe/STO have the same form as given by the expressions (3- 5) with the difference that the parameters κ_0 and κ_∞ must be redefined to account for the inevitable change in the dielectric characteristics of the $SrTiO_3$ surface after annealing and deposition of the FeSe-layer . Therefore, in what follows, in all expressions $\tilde{\kappa}_0$ and $\tilde{\kappa}_\infty$ are the model parameters that may depend on details of the specific experiment.

We return to the expression of the matrix element for scattering of two electrons by each other via virtual exchange of the surface LO phonon. Together with the term corresponding to common scattering of two electrons via the direct electron-electron Coulomb interaction, the total matrix element (4) acquires the form:

$$\mathrm{M}_{tot}(\vec{p},\varepsilon_n \mid \vec{k},\varepsilon_m) = \frac{4\pi e^2}{(\tilde{\kappa}_\infty + 1)q} - \sum_i \frac{4\pi e^2}{q(\tilde{\kappa}_\infty + 1)} V_i^2 \times D_{SLO}^i(\varepsilon_n - \varepsilon_m). \quad (6)$$

Summation is on the number N of optical phonons in the system. We assume $N = 3$, because there are *three* infrared-active LO phonon modes at the Γ-point of bulk $SrTiO_3$ [18], each with a frequency $\omega_{LO}^i > T_C$ [19]. The factor V_i^2 accounts for the property that in multi-mode polar crystals coupling of the optical phonons with electrons generally differs from that in Eq. (4) and the coefficients V_i^2 have a more complicated form than in (4, 5). Nevertheless, in $SrTiO_3$ among all phonon modes, one LO mode exhibits a giant gap between its frequency and the frequencies of all the transverse optical (TO) phonons [17, 19]. Therefore, the contribution from this mode into (6) can be taken as before in the same form as in Eq. (4). In particular, it compensates the direct Coulomb repulsion in Eq. (6) at $|\varepsilon_n - \varepsilon_m| << \omega_{LO}$.

The rest of the LO phonons in (6) contribute to the matrix element for electron-electron scattering. We emphasize that the latter corresponds to the *attractive* interaction. Besides, as κ_0 of $SrTiO_3$is very large ($\kappa_0 >> \kappa_\infty$ [18]), we retain in the denominators (6) only the terms with an "optical" $\tilde{\kappa}_\infty + 1$.

We apply these considerations to the interaction between the band electrons in the FeSe layer and the LO phonons at the 1UCFeSe/STO interface. With the simplifying assumption of the *extreme* "anti-adiabatic" case, $\omega_0 >> E_F$, the term $(\varepsilon_n - \varepsilon_m)^2$ in the denominator of $D_{SLO}^i(\varepsilon_n - \varepsilon_m)$ can be omitted.

The matrix element of the interaction between the two electrons in the FeSe conduction band becomes:

$$\mathrm{M}_{tot}(\vec{p},\varepsilon_n \mid \vec{k},\varepsilon_m) \equiv M(\vec{p}-\vec{k}) \approx -2\alpha^2 \frac{4\pi e^2}{\mid \vec{p}-\vec{k} \mid (\tilde{\kappa}_\infty + 1)} < 0 . \quad (7)$$

Here the notation $2\alpha^2$ is introduced for the sum of V_i^2 over all other LO phonon modes; $\alpha^2 < 1$ is one of the parameters in the model; the second parameter is $\tilde{\kappa}_\infty$ -the optical dielectric constant renormalized by the presence of electrons embedded into the interface layer.

The Coulomb interaction is screened by the two-dimensional gas of FeSe-electrons. Restricting ourselves to the so-called random phase approximation (RPA), the denominator in (7) becomes:

$$\mid \vec{p}-\vec{k} \mid \Rightarrow \mid \vec{p}-\vec{k} \mid + 4e^2 m / \hbar(\bar{\kappa}_\infty + 1) . \quad (8)$$

Instead of (7), one obtains:

$$M_{scr}(\vec{p}-\vec{k}) \approx -2\alpha^2 \frac{4\pi e^2}{\tilde{\kappa}_\infty} \times \frac{1}{\mid \vec{p}-\vec{k} \mid + 4e^2 m / \hbar(\bar{\kappa}_\infty + 1)} . \quad (9)$$

Generally, the 2D-screening depends on many structural details of the conducting layer [20]. Use of RPA-type expressions (8, 9) can be justified in the "dense plasma" limit, i.e., when the kinetic energy of carriers prevails over the Coulomb interaction. In that case the inverse Thomas-Fermi radius $k_{TF} \equiv r_{TF}^{-1}$ must be small compared with the characteristic momentum p_F . For the former from Eq. (8) one finds $k_{TF} = 4e^2 m / \hbar(\bar{\kappa}_\infty + 1)$. For the experiments of interest, the following inequality holds:

$$p_F(\hbar(\bar{\kappa}_\infty + 1) / e^2 m) >> 1 . \quad (10)$$

Weak-coupling expression for the superconducting transition temperature. The temperature of the superconducting transition is determined by the eigenvalue of the homogeneous equation for the gap parameter $\Delta(\vec{p})$ (see [16] and the brief derivation in the Appendix). In the notation of (9) it is:

$$\Delta(\vec{p}) = -T \sum_m \int \frac{d\vec{k}}{(2\pi)^2} M_{scr}(p-k)\Pi(k)\Delta(\vec{k}) . \quad (11)$$

The Cooper instability originates from the logarithmic divergence related to blocks of the two Green functions $\Pi(k) \equiv G(k)G(-k) = [\varepsilon_m^2 + \varsigma^2]^{-1}$ in (11). (From now on $\varsigma = (\vec{k}^2 - p_F^2)/2m \approx v_F(k - p_F)$). As was pointed out above, at $\omega_{SLO} >> E_F$, the dependence on the energy variable in (5) can be omitted so that $\mathrm{M}_{scr}(\vec{p},\varepsilon_n \mid \vec{k},\varepsilon_m) \Rightarrow M_{scr}(\vec{p}-\vec{k})$. Performing the summation in (11) and substituting the explicit expression (9) for the integral kernel $M_{sc}(\vec{p}-\vec{k})$ results in the integral equation:

$$\Delta(\vec{p}) = \frac{2\alpha^2 e^2 m}{\pi\tilde{\kappa}_\infty} \int_{-\pi}^{\pi} \int_0^\infty \frac{d\varphi d\varsigma}{\mid \vec{p}-\vec{k} \mid + 4e^2 m / \hbar(\bar{\kappa}_\infty + 1)} \times \frac{1}{\varsigma} th\frac{\varsigma}{2T} \Delta(\vec{k}) . \quad (12)$$

(φ is the angle between two vectors $\vec{p}$ and $\vec{k}$).

Let the vector $\vec{p}$ in (12) be *on the Fermi surface*. With the notation $\bar{\Delta}$ for the average value of $\Delta(k)$, rewrite the right hand side of (12) as:

$$\frac{2\alpha^2 e^2 m}{\pi\tilde{\kappa}_\infty}\int_{-\pi}^{\pi}\int_0^W \frac{d\varsigma}{\varsigma} th\frac{\varsigma}{2T}\times\frac{d\varphi}{\sqrt{2p_F^2(1-\cos\varphi)+2m\varsigma+4e^2m/\hbar(\bar{\kappa}_\infty+1)}}\Delta(k)\Rightarrow\lambda\ln\left(\frac{W}{T}\right)\bar{\Delta}. \quad (13)$$

The integral over the angle φ in front of the logarithmic singularity in Eq. (13) at $\varsigma=0$ determines the exponential factor in the weak coupling expression $T_C = const\times W(2\gamma/\pi)\exp(-1/\lambda)$ for the transition temperature. In (13) W is a characteristic energy scale. That is, if the interaction kernel decreases at large energies, W is the order-of-magnitude cutoff parameter in the integration over ς on the left in Eq. (13). (Strictly speaking, $\Delta(k)$ also depends on the energy variable ς_k). In our example of the *extreme* "anti-adiabatic" case $\omega_0 >> E_F$ it is self-evident that $W = const\times E_F$. (The *exact* value of $const\sim 1$ can be determined only by solving the integral equation (12) explicitly).

Defining the effective Bohr radius $\bar{a}_B = (\bar{\kappa}_\infty+1)\hbar^2/e^2m$, inequality (10) becomes in this new notation:

$$p_F\bar{a}_B >> 1. \quad (14)$$

Introducing the dimensionless parameter $x = (p_F\bar{a}_B/\hbar)/2$ and with the λ in Eq. (13) written as $\lambda\equiv\alpha^2\lambda(x)$ one obtains:

$$\lambda(x) = \frac{2}{\pi}\int_0^{\pi/2}\frac{du}{x\sin u+1}. \quad (15)$$

For the transition temperature:

$$T_C(x) = const\times(p_F^2/2m)\exp[-1/\alpha^2\lambda(x)] \equiv const\times(2\hbar^2/m\bar{a}_B^2)x^2\exp[-1/\alpha^2\lambda(x)]. \quad (16)$$

For illustration purpose, take $\alpha^2=1$. The two functions $\lambda(x)$, and $t(x)=x^2\exp[-1/\lambda(x)]$ are plotted in Fig. 1a, b. The maximum in $t(x)$ is obviously due to competition between two factors: at a given $\bar{a}_B$ the transition temperature initially increases with an increase in carriers concentration; at the same time, screening tends to reduce the effective interaction constant $\lambda(x)$.

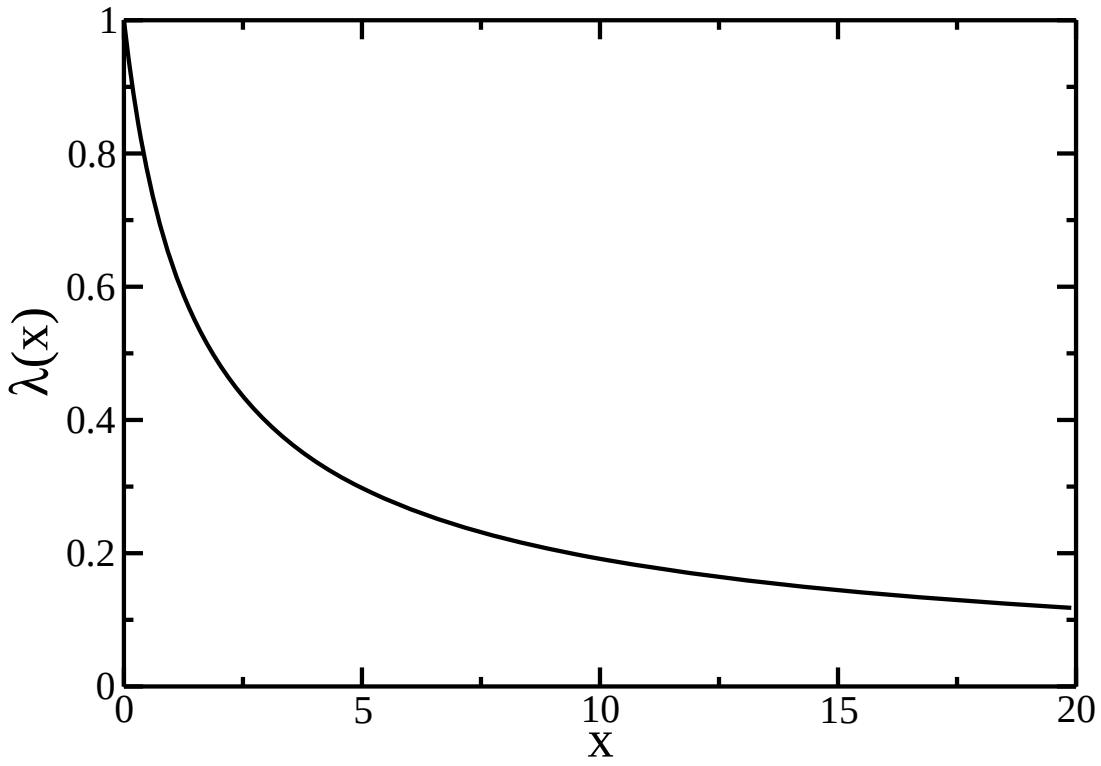

Fig.1a. The exponential factor in the weak coupling expression $T_c = const \times W \exp[-1/\lambda(x)]$ for the transition temperature, $\lambda(x)$ Eq. (15) as function of the dimensionless parameter $x = p_F \bar{a}_B / 2\hbar$; (p_F -the Fermi momentum; $\bar{a}_B = (\bar{\kappa}_\infty + 1)\hbar^2 / e^2 m$ -the effective Bohr radius).

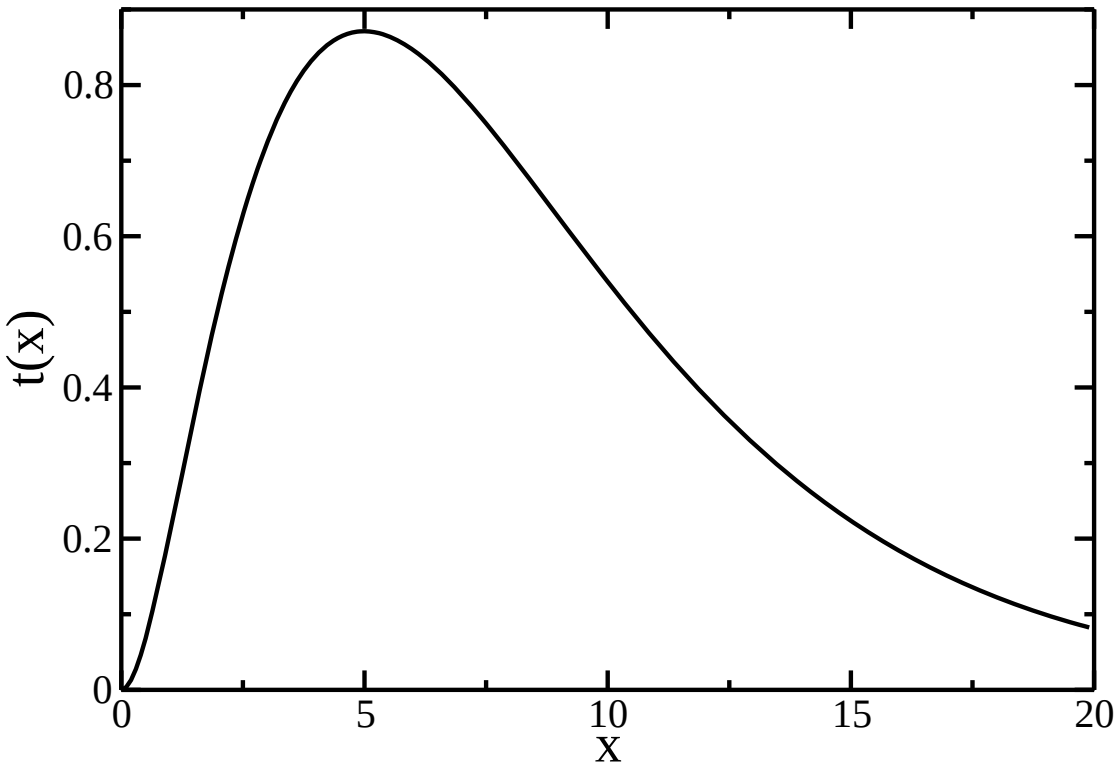

Fig.1b. The function $t(x) = x^2 \exp[-1/\lambda(x)]$. See expression (16) for the superconducting transition temperature $T_C(x) = const \times (p_F^2 / 2m) \exp[-1/\lambda(x)] \equiv const \times (2\hbar^2 / m\bar{a}_B^2) t(x)$.

Replica bands. The intensity of the ARPES spectra is proportional to the spectral function $A(\varepsilon, \vec{p})$ related to the imaginary part of the retarded Green function $G_R(\vec{k};\omega) = [\omega - \varepsilon(\vec{k}) + \mu - \Sigma(\vec{k};\omega)]^{-1}$ as:

$$A(\varepsilon, \vec{p}) = -\frac{1}{\pi} \frac{\mathrm{Im}\,\Sigma(\varepsilon, \vec{p})}{[\varepsilon - \varepsilon(\vec{k}) + \mu - \mathrm{Re}\,\Sigma(\varepsilon, \vec{p})]^2 + [\mathrm{Im}\,\Sigma(\varepsilon, \vec{p})]^2} . \qquad (17)$$

In the general expression (17) for $A(\varepsilon, \vec{p})$ we confine ourselves to the intermediate states with one optical phonon. Correspondingly, for the self-energy in (17) we consider the diagram containing only one line of the phonon Green function. The analytical continuation of the expression $\Sigma(\varepsilon, \vec{p})$:

$$\Sigma(\varepsilon, \vec{p}) = -T \sum_m \int \frac{d\vec{k}}{(2\pi)^2} M_{sc}(\vec{k}) G(\vec{p} - \vec{k}, \varepsilon - \varepsilon_m) D_{SLO}(\vec{k}, \varepsilon_m) \quad (18)$$

on the thermodynamic axis to the real frequency axis defines the retarded self-energy part $\Sigma_R(\varepsilon, \vec{p})$ as (see [16]):

$$\Sigma_R(\varepsilon, \vec{p}) = -\frac{1}{(2\pi)^3 \pi} \int d^2\vec{k} M_{scr}(\vec{k}) \int_{-\infty}^{+\infty} d\omega \int_{-\infty}^{+\infty} d\varepsilon_1 \frac{\mathrm{Im}\,G_R(\varepsilon_1, \vec{p} - \vec{k})\,\mathrm{Im}\,D_R(\omega, \vec{k})}{\omega + \varepsilon - \varepsilon_1 - i\delta} \times [\tanh\frac{\varepsilon_1}{2T} + \coth\frac{\omega}{2T}] \quad (19)$$

Making use of the expressions for $\mathrm{Im}\, D(\omega,\vec{k}) = -\pi(\omega_{SLO}/2)\{\delta(\omega-\omega_{SLO})-\delta(\omega+\omega_{SLO})\}$ and for $\mathrm{Im}\, G_R(\varepsilon,\vec{p}) = -\pi\delta(\varepsilon-\varepsilon(\vec{p})+\mu)$, one obtains:

$$\Sigma_R(\varepsilon,\vec{p}) = \frac{\omega_{SLO}}{2^4\pi^2}\int d^2\vec{k} M_{scr}(\vec{k}) \frac{1}{\omega_{SLO}-\varepsilon+\varepsilon(\vec{p}-\vec{k})-\mu+i\delta} \times[\tanh\frac{\mu-\varepsilon(\vec{p}-\vec{k})}{2T}+\coth\frac{\omega_{SLO}}{2T}]. \quad (20)$$

At low temperatures $T << E_F, \omega_{SLO}$ Eq. (20) simplifies to:

$$\mathrm{Im}\,\Sigma_R(\varepsilon,\vec{p}) = -(\omega_{SLO}/2^3\pi)\int d^2\vec{k} M_{scr}(\vec{k})\delta(\omega_{SLO}-\varepsilon+\varepsilon(\vec{p}-\vec{k})-\mu). \quad (21)$$

In practice, to improve resolution, the weak-intensity bands are usually analyzed by taking the second derivatives of the ARPES spectra. Following [4], consider the second derivative $(\partial^2/\partial\varepsilon^2)[\mathrm{Im}\,\Sigma_R(\varepsilon,\vec{p})]$ of Eq.(21). Rewriting $(\partial/\partial\varepsilon)\delta(\omega_{SLO}-\varepsilon+\varepsilon(\vec{p}-\vec{k})-\mu)$ as $-(1/v_x(\vec{p}-\vec{k}))(\partial/\partial k_x)\delta(\omega_{SLO}-\varepsilon+\varepsilon(\vec{p}-\vec{k})-\mu)$, repeating: $(\partial/\partial\varepsilon)\to -[1/v_y(\vec{p}-\vec{k})](\partial/\partial k_y))$, and leaving after the integration by parts only the most singular terms in $M_{scr}(\vec{k})$ Eq. (9), we find:

$$\frac{\partial^2}{\partial\varepsilon^2}\mathrm{Im}\,\Sigma_R(\varepsilon,\vec{p}) = -\frac{4\pi\omega_{SLO}e^2}{\tilde{\kappa}_\infty}\int\frac{kdk}{v^2(\vec{p}-\vec{k})}\times\frac{\delta(\varepsilon+\mu-\omega_{SLO}-\varepsilon(\vec{p}-\vec{k}))}{\{k+4e^2m/\hbar(\bar{\kappa}_\infty+1)\}^3}. \quad (22)$$

Assuming the integral converges at $4e^2m/\hbar(\bar{\kappa}_\infty+1) = 4\hbar/\bar{a}_B << p_F$ one finally obtains:

$$\frac{\partial^2}{\partial\varepsilon^2}\mathrm{Im}\,\Sigma_R(\varepsilon,\vec{p}) = -\frac{\pi\omega_{SLO}}{2v^2(\vec{p})m}\delta(\varepsilon+\mu-\omega_{SLO}-\varepsilon(\vec{p})). \quad (23)$$

Discussion. The experimental facts available thus far [1, 2, 5-8] are not specific enough to admit a detailed comparison with the theoretical results above, the more so, as no *quantitative* measurements of the dependence of T_C on the carrier concentration at the single-layer FeSe/STO were established with any degree of confidence (see e.g. [6-8]; the field effect has been observed in [6]).

The possibility for a more quantitative discussion presents itself in connection with the question regarding the origin of replicas [4].

There are two independent physical characteristics beside α^2 that enter into the theoretical expressions (7, 9, 12 and 13): p_F and the effective Bohr radius $\bar{a}_B = e^2m/\hbar^2(\bar{\kappa}_\infty+1)$. The values of p_F are available directly from the ARPES spectra and define the surface density of electrons $n_s = (p_F^2/2\pi\hbar^2)$. The effective Bohr radius (and, hence, $\bar{\kappa}_\infty$) will be now evaluated indirectly making use of the ARPES measurements[4].

It was stressed in [4] that to account for the very accurate one-to-one correspondence between the dispersion of the electron energy bands and that of the replicas, especially at the M-point of the BZ, the electron-phonon interaction must be peaked at small momentum transfer $|\vec{q}|$. Compare now $q_0 \approx 0.1\times10^8\, cm^{-1}$, the experimental error for the replica-widths [4], with the value of cutoff $4e^2m/\hbar(\bar{\kappa}_\infty+1) = 4\bar{a}_B^{-1}\hbar$ in the denominator of Eq. (22). Comparison gives $4\bar{a}_b^{-1} \square q_o$, or

$\bar{a}_B \approx 40\times10^{-8} cm$. With the band mass $m \approx 2m_e$ from [4] one finds $(\bar{\kappa}_\infty + 1) \approx 160$ (in the *dielectric* $SrTiO_3$ $\kappa_\infty \approx 5.2$ [18]).

On substitution of $p_F / \hbar \approx 0.3\times10^8 cm^{-1}$, the dimensionless parameter becomes $x = (p_F \bar{a}_B / \hbar)/2 = 6$. The inequality (14) is fulfilled when $p_F \bar{a}_B / \hbar = 12 >> 1$. Because of this, the applicability of the approach to the analysis above is justified.

From here one now obtains $\lambda(6) \approx 0.25$ (see Fig.1a). The substitution of this value into Eq. (15) leads to $T_C(x) \approx const \times E_F \times 0.02 = const \times 12K$ ($E_F \approx 60meV$ [4, 9]). Therefore, assuming $const \approx 1$, the interaction of electrons with LO optical phonons *alone* cannot account for $T_C = 58 \pm 7K$ reported in [4].

If there are *two* mechanisms contributing to the Cooper pairing, the gap equations (12, 13) must be rewritten:

$$\Delta(\vec{p}) = \int_0^{\tilde{E}} K(p,k) \frac{d\varsigma_k}{\varsigma_k} th\frac{\varsigma_k}{2T} \Delta_1(\vec{k}) + \frac{2\alpha^2 e^2 m}{\pi\tilde{\kappa}_\infty} \int_{-\pi}^{\pi}\int_0^{\infty} \frac{d\varphi d\varsigma}{|\vec{p}-\vec{k}| + 4e^2 m/\hbar\bar{\kappa}_\infty} \times \frac{1}{\varsigma} th\frac{\varsigma}{2T} \Delta(\vec{k}) \quad . \quad (24)$$

In (24) $K(p,k)$ is now the kernel related to that specific pairing mechanism that, hypothetically, supports superconductivity in bulk FeSe. One view popular in the literature is that superconducting pairing in bulk FeSe is mediated by antiferromagnetic fluctuations (see, for instance, [13]). In the case of such a mechanism the characteristic cutoff energy in the first integral to an order of magnitude should be the same $\tilde{E} \sim E_F$. Assuming the weak-coupling expression $T_{C0} \approx E_F \exp(-1/\nu)$ in bulk FeSe, with $T_{C0} \approx 8K$ and $E_F \approx 650K$ one finds from this $\nu = [\ln(E_F / T_{C0})]^{-1} \approx 0.23$. Inserting $\lambda(x) \approx 0.25$ and $\nu \approx 0.23$ gives the total $\lambda_{tot} \approx 0.48$ in the exponent; upon substitution into $T_C \approx E_F \exp(-1/\lambda_{tot})$ one finds for T_C a reasonable estimate $T_C(x) \approx const \times 88K$.

If, instead being of magnetic origin, $T_{C0} \approx 8K$ in bulk FeSe could be caused by a commonplace phonon pairing with the Debye temperature $\theta_D \approx 200K$, for ν it would follow that $\nu = [\ln(\theta_D / T_{C0})]^{-1} \approx 0.31$. As $\theta_D << E_F$, in this case Eq. (24) must be solved separately for $\Delta(\vec{k})$ in the two energy intervals $[0, \theta_D]$ and $[\theta_D, E_F]$. Simple calculations lead to the renormalized $\lambda_{ren}(x) = \lambda(x)[1 - \lambda(x)\ln(E_F / \theta_D)]^{-1} \approx 0.36$ and to $\lambda_{tot} \approx 0.67$; one then finds $T_C \approx const \times \theta_D \exp(-1/\lambda_{tot}) = const \times 45K$.

These estimates, although crude for ultimatequantitative conclusions, do not contradict the possibility that the record $T_C \approx 109K$ [2] may be explained as caused by the enhancement of the bulk $T_{C0} \approx 8K$. On the theory side, it would be enough, as an example, to assume $x = (p_F \bar{a}_B / 2\hbar) \approx 4$ and $\lambda(4) \approx 0.32$ (see Fig. 1a). Note in passing that the value of $p_F \bar{a}_B / \hbar \approx 8$ would satisfy the inequality (14) as well.

With two independent parameters p_F and $\bar{a}_B$ there is only one dimensionless parameter in the theory $x = p_F \bar{a}_B / 2\hbar$. Post factum, from the above discussion one concludes that in the main part of the $(p_F, \bar{a}_B)$-phase diagram in Fig.1a, b the use of RPA in Eqs. (8, 9) is warranted by the inequality (14). (Thus, a maximum of the function $t(x) = x^2 \exp[-1/\lambda(x)]$ in Fig.1b is at $x \approx 5$ ($p_F \bar{a}_B / \hbar \approx 10$)). At the level of current experiments [4] it may be possible to test Eq. (23). Namely, the second derivative

of the replica band intensity (23) does not depend on x while $T_C(x)$ decreases with increasing x (recall that ARPES can directly measure p_F).

The second parameter $(\bar{\kappa}_\infty + 1)$, intuitively, seem to be related to the particulars of the sample preparation procedure. At fixed $x = p_F \bar{a}_B / 2\hbar \approx 6$ [4], reduction of $\bar{a}_B$, say, by a factor of three $(\bar{a}_B \to \bar{a}_B / 3)$ leads to $T_c = const \times 108K$ in Eq. (16). For that density $n_s \approx 1.4 \times 10^{14} cm^{-3}$ in [4] must be increased to $n_s \approx 1.3 \times 10^{15} cm^{-3}$. This formal example is, however, an illustration that by establishing better control of doping one may manipulate the superconducting properties of the single-layer FeSe/STO.

In summary, we point out that with the sample preparations methods accepted in the current experimental literature the two-dimensional system of charges at the FeSe/$SrTiO_3$ interface inevitably includes both itinerant and immobile electrons. Electrons trapped below the mobility edge are responsible for the change of the dielectric constant at the substrate surface. The Cooper pairing matrix elements in single-layer FeSe/STO are calculated in the model of band electrons interacting with the electric potential of a longitudinal (LO) phonon mode at the $SrTiO_3$ surface. The dielectric constant at the surface is the free parameter of the model. HERE

It is shown that the theoretical results are applicable over the entire range of typical experimental parameters. In particular, screening of the Coulomb interaction can be accounted for in the random phase approximation. The estimates for the superconducting transition temperature lead to the conclusion that the LO-phonon mediated pairing alone cannot account for superconductivity at the temperatures reported, for instance, in [4]. The conclusion, however, may not be the ultimate one, as the general theoretical expressions do not contradict the possibility that with better control of doping one can enhance further the superconducting properties of 1uCFeSe/STO.

ACKNOWLEDGMENTS

The author thanks T. Siegrist and C. Beekman for many helpful discussions and for the clarification of a number of significant experimental details and A. Migliori for reading the manuscript carefully and for his comment . I am grateful to H. J. Mard for creating the graphic material. The work is supported by the National High Magnetic Field Laboratory through NSF Grant No. DMR-1157490, the State of Florida and the U.S. Department of Energy.

Appendix

The onset of superconductivity at the temperature of transition T_C manifests itself in the occurrence of the pole in the scattering amplitude of two electrons with zero total momentum and frequency [23]. In the notation $\Gamma(p,-p \mid p',-p') \equiv \Gamma(p \mid p')$ the amplitude is the sum of all diagrams in the Cooper channel:

$$\Gamma(p,\mid p') = M(p-q) - \frac{T}{(2\pi)^2} \Sigma_{n'} \int d\vec{k} M(p-k) G(k) G(-k) \Gamma(k,\mid p') \ .$$

The superconducting transition temperature is determined via the eigenvalue of the following homogeneous equations. Substitution $\Gamma(p,|\, p') \to \psi(p)$ leads to the integral equation for a function $\psi(p)$:

$$\psi(p) = -T\sum_m \int \frac{d\vec{k}}{(2\pi)^2} M(p-k)\Pi(k)\psi(k)\,.$$

References

[1] Q. -Y. Wang, Z. Li, W. -H. Zhang, Z. -C. Zhang, J.-S. Zhang, W. Li, H. Ding, Y. -B. Ou, P. Deng, K. Chang, J. Wen, C. -L. Song, K. He, J. -F. Jia, S. -H. Ji, Y. -Y. Wang, L. -L. Wang, X. Chen, X. -C. Ma, and Q. -K. Xue, Chin. Phys. Lett. **29**, 037402 (2012)
[2] J. -F. Ge, Z. -L. Liu, C. Liu, C. -L. Gao, D. Qian, Q. -K. Xue, Y. Liu, and J. -F. Jia, Nat. Mater. **14**, 285(2015)
[3] P. B. Allen and R. C. Dynes, Phys. Rev. B**12**, 905 (1975)
[4] J. J. Lee, F. T. Schmitt, R. G. Moore, S. Johnston, Y. -T. Cui, W. Li, M. , Z. K. Liu, M. Hashimoto, Y. Zhang, D. H. Lu, T. P. Devereaux, D. -H. Lee, and Z. -X. Shen, Nature, **515**, 245 (2014)
[5] R. Peng, H.C. Xu, S.Y. Tan, H.Y. Cao, M. Xia X.P. Shen, Z.C. Huang, C.H.P. Wen, Q. Song,T. Zhang, B.P. Xie, X.G. Gong, and D.L. Feng, Nat. Commun.**5**, 5044 (2014)
[6] W. Zhang, Z. Li, F. Li, H. Zhang, J. Peng, C. Tang, Q. Wang, K. He, X. Chen, L. Wang, X. Ma, and Q. -K. Xue, Phys. Rev. B **89**, 060506(R) (2014)
[7] X. Liu, D. Liu, W. Zhang, J. He, L. Zhao, S. He, D. Mou, F. Li, C. Tang, Z. Li, L. Wang, Y. Peng, Y. Liu, C. Chen, L.Yu, G.Liu, X. Dong, J. Zhang, C. Chen, Z. Xu, X. Chen, X. Ma, Q. Xue, and X.J. Zhou, , Nature Comm. **5**, 5047, 1(2014)
[8] J. He, X. Liu, W. Zhang, L. Zhao, D. Liu, S. He, D. Mou, F. Li, C. Tang, Z. Li, L. Wang, Y. Peng, Y. Liu, C. Chen, L. Yu, G. Liu, X. Dong, J. Zhang, C. Chen, Z.Xu, X. Chen, X. Ma, Q. Xue, and X. J. Zhou, PNAS **111**, 18501(2014)
[9] D. Liu, W. Zhang, D. Mou , J. He, Y.-B. Ou, Q.-Y.Wang, Z. Li, L. Wang, L. Zhao, S. He, Y. Peng, X. Liu, C. Chen, L. Yu, G. Liu, X. Dong, J. Zhang, C. Chen, Z. Xu, J. Hu, X. Chen, X. Ma, Q. Xue, and X.J. Zhou, Nat. Commun.**3**, 931 (2012)
[10] F. Zheng, Z. Wang, W. Kang, and P. Zhang, Sci. Reports, **3**, 02213 (2013)
[11] S. Q. Wang and G. D. Mahan, Phys. Rev. B **6**, 4517 (1972)
[12] Y. -Y. Xiang, F. Wang, D. Wang, Q.-H. Wang, and D.-H. Lee, *High-temperature superconductivity at the FeSe/SrTiO3 interface*, Phys. Rev. B **86**, 134508 (2012)
[13] D. -H. Lee, arXiv: 1508.02461v1 (2015)
[14] G.M. Eliashberg, Sov. Phys. JETP **11**, 696 (1960)
[15] A. B. Migdal, Sov. Phys. JETP **7**, 996 (1958)
[16] A. A. Abrikosov, L. P. Gor'kov, and I. E. Dzyaloshinskii, *Methods of Quantum Field Theory in Statistical Physics,* Prentice-Hall, Inc., Englewood Cliffs, New Jersey, 1963
[17] K. A. Muller and H. Bukard, Phys. Rev. B **19**, 3593 (1979)
[18] W. Zhong, R.D. King-Smith, and D. Vanderbilt, Phys. Rev. Lett.**72**, 3618 (1994)
[19] N. Choudhury, E. J. Walter, A. I. Kolesnikov, and C.-K. Loong, Phys. Rev. B 77,134111 (2008)
[20] F. Stern, Phys. Rev. Lett. **18**, 546 (1967)